CRISP-contourlets: a critically sampled directional multiresolution image representation

Yue Lu and Minh N. Do

Department of Electrical and Computer Engineering
University of Illinois at Urbana-Champaign, Urbana IL 61801, USA

ABSTRACT

Directional multiresolution image representations have lately attracted much attention. A number of new systems, such as the *curvelet* transform and the more recent *contourlet* transform, have been proposed. A common issue of these transforms is the redundancy in representation, an undesirable feature for certain applications (e.g. compression). Though some critically sampled transforms have also been proposed in the past, they can only provide limited directionality or limited flexibility in the frequency decomposition. In this paper, we propose a filter bank structure achieving a nonredundant multiresolution and multidirectional expansion of images. It can be seen as a critically sampled version of the original contourlet transform (hence the name *CRISP-contourets*) in the sense that the corresponding frequency decomposition is similar to that of contourlets, which divides the whole spectrum both angularly and radially. However, instead of performing the multiscale and directional decomposition steps separately as is done in contourlets, the key idea here is to use a combined iterated non-separable filter bank for both steps. Aside from critical sampling, the proposed transform possesses other useful properties including perfect reconstruction, flexible configuration of the number of directions at each scale, and an efficient tree-structured implementation.

Keywords: Multiresolution, multidirectional, filter banks, image representation, maximal decimation

1. INTRODUCTION

If asked to identify a "wish list" for a new efficient image representation,[1] we would put *multiresolution*, *localization*, *directionality*, *critical sampling*, *anisotropy*, and *efficient implementation* on top of the list. The first three requirements were suggested by studies related to the human visual system[2,3] and natural image statistics.[4] In particular, multiresolution asks for the image be successively approximated, from a coarse version to finer details; localization means the basis elements in the representation should be localized in both the spatial and frequency domains; directionality requires the representation have a high angular resolution, containing elements oriented at a large number of different directions. For some applications (e.g. compression), nonredundant representation is essential, thus we also put critical sampling in the list. In this case, the representation will span a basis of the image space. To capture smooth contours in images, the support size of the representation elements should also obey the *anisotropy scaling law*[5] for curves: $width \propto length^2$. Last but not least, an efficient implementation is essential for any practical systems.

A number of image representations have been proposed in the literature, each satisfying several, but not all, of the above objectives. Candès and Donoho[5,6] pioneered a new multiscale and directional expansion, called *curvelets*, that is shown to achieve optimal approximation behavior in a certain sense for 2-D piecewise smooth functions. One of the key features of curvelets is their support sizes obey the anisotropy scaling law mentioned above. Originally developed in the continuous domain, the curvelet constructions require a rotation transform, which makes the implementation of the transform on discrete images very challenging. Meanwhile, curvelet transform is a redundant representation for images.

Several other well-known systems include the *directional wavelets*[7,8] and the *complex wavelets*,[9] to name a few. A nice thing about these systems is that they can be implemented rather efficiently using a tree-structured

Further author information:
Yue Lu: yuelu@uiuc.edu; Minh N. Do: minhdo@uiuc.edu

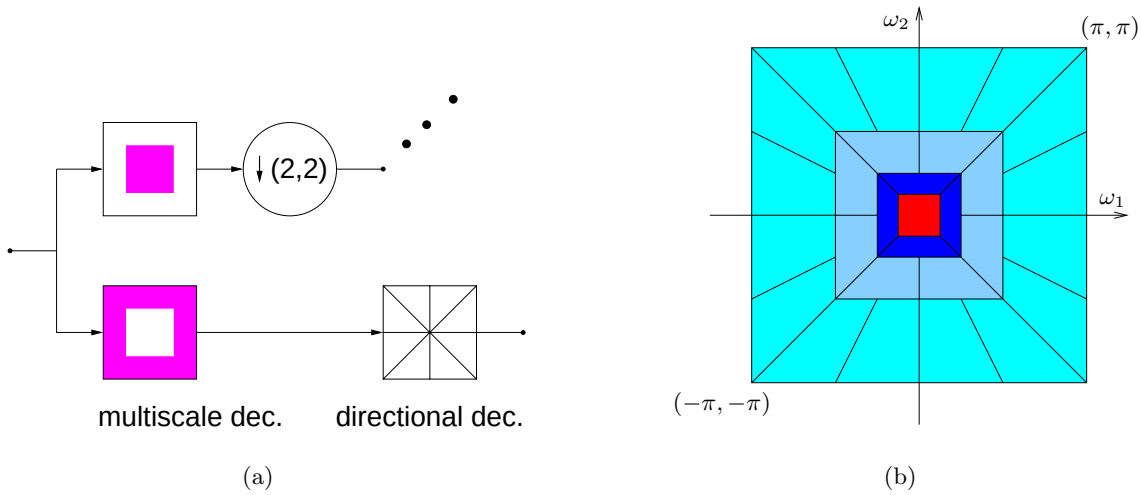

Figure 1. The contourlet transform. (a) Block diagram. It uses an iterated combination of the Laplacian pyramid and the directional filter bank. (b) Resulting frequency division, where the whole spectrum is divided both angularly and radially and the number of directions is increased with frequency.

construction. However, they can only provide limited directionality and do not allow for a different number of directions at each scale.

More recently, Do and Vetterli[1, 10] proposed a computational framework, called *contourlets*, for the directional multiresolution representation of discrete images. As shown in Fig.1(a), the contourlet transform employs an efficient tree-structured implementation, which is an iterated combination of the Laplacian pyramid and the directional filter bank.[11] Meanwhile, it has a desirable frequency decomposition, where the whole spectrum is divided both angularly and radially. It can be shown that the contourlet transform achieve most of the objectives in our "wish list". Actually the only thing left is critical sampling, which is due to the use of the Laplacian pyramid. A redundancy rate of up to 4/3 is brought into the system.

The purpose of this paper is to introduce a new directional multiresolution image representation that can achieve a similar frequency decomposition to that of contourlets, while with a nonredundant expansion. In principle, this new system can be seen as a critically sampled version of the original contourlets transform, and hence is named *CRISP-contourlets*. Instead of performing the multiscale and directional decomposition steps independently as in contourlets, the key idea here is to use a combined iterated nonseparable filter bank for both steps. Fig. 2 shows a typical frequency decomposition of CRISP-contourlets. Here we have four lowpass regions, denoted as 0, 1, 2, 3 in the figure. Starting from the second level, the number of directions is doubled with the increase of frequency. In particular, each bandpass region can have 3×2^n $(n = 2, 3, \ldots)$ directions. The similarity in frequency division allows for the new system to inherit the merits of the contourlet transform. While the added feature of nonredundant representation makes it a potentially more promising system for applications like compression.

In a similar effort, Hong and Smith[12] proposed an octave-band family of nonredundant directional filter banks (OBDFB), which also achieves a certain radial and directional decomposition of the spectrum. Aside from the difference in the shapes of directional bandpass regions, our system allows more flexibility in the number of directions at each band. As a special case (not shown in Fig. 2), CRISP-contourlets can also double the numbers of directions at every other multiscale level, which is similar to the contourlets.

The outline of the paper is as follows. Section 2 introduces several results in 2-D multirate systems that serves as background and provides intuitions for the design of the new system. Section 3 concentrates on the details of the CRISP-contourlet transform, including the specific filter banks used and the iterated expansion rule. In Section 4 we design the FIR filters used in the system.

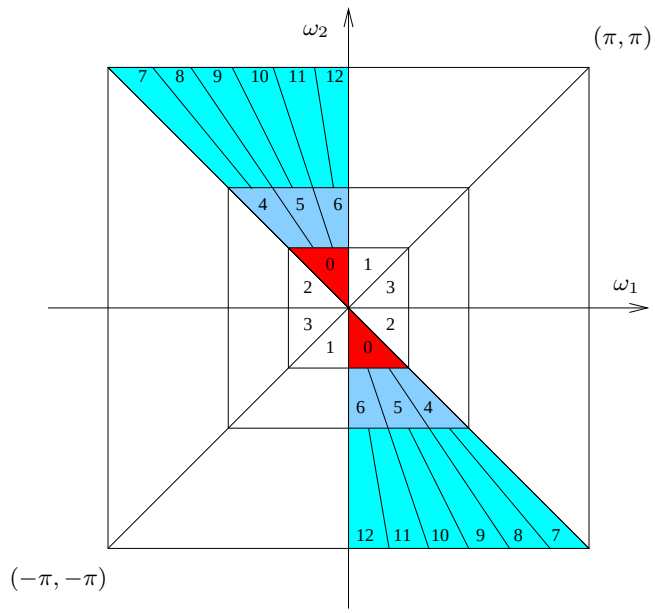

Figure 2. A typical frequency decomposition of the CRISP-contourlet transform. For the sake of clarity, we only show the details of frequency division in the gray area. The division in other areas can be got via symmetry. In CRISP-contourlets, we have four lowpass regions, denoted as 0, 1, 2, 3. The number of directions is increased with frequency. In particular, each bandpass region can have 3×2^n $(n = 2, 3, \ldots)$ directions.

2. MAXIMALLY DECIMATED FREQUENCY SUPPORT

The theory of multidimensional multirate systems has been extensively studied in the past. Excellent tutorials on this topic can be found in references.[13–15] In this section, we will review several important results, which not only lay the ground for the following discussion, but also reveal the important intuitions in the CRISP-contourlets system.

Let $x(\boldsymbol{n})$ be a 2-D discrete signal and $y(\boldsymbol{n})$ be the decimated version of $x(\boldsymbol{n})$ through a nonsingular matrix $\boldsymbol{M}$, i.e. $y(\boldsymbol{n}) = x(\boldsymbol{M}\boldsymbol{n})$. The relationship between the two signals in the Fourier domain can be expressed as:[14]

$$Y(\boldsymbol{\omega}) = \frac{1}{\mu} \sum_{l=0}^{\mu-1} X(\boldsymbol{M}^{-T}(\boldsymbol{\omega} - 2\pi \boldsymbol{k}_l)), \tag{1}$$

where $X(\boldsymbol{\omega})$, $Y(\boldsymbol{\omega})$ are the Fourier transform of the corresponding signals, $\mu = |det(\boldsymbol{M})|$, and $\{\boldsymbol{k}_l\}_{l=0}^{\mu-1}$ are the coset vectors of $\boldsymbol{M}^T$.

We will first restrict our attention to the case of ideal signals, where $X(\boldsymbol{\omega}) = 1$ in its passband and 0 elsewhere. The issue of designing FIR filters approximating the ideal supports will be discussed in Section 4. For now, the signals are solely specified by the shapes of their frequency supports and it is convenient to introduce the following notion.

For any ideal spectrum $X(\boldsymbol{\omega})$, we use the point set $\mathcal{X} \triangleq \{\boldsymbol{\omega} : \boldsymbol{\omega} \in \text{support of X}(\boldsymbol{\omega})\}$ to represent its support region. Note that $\mathcal{X}$ is periodic with an interval $2\pi \times 2\pi$. Let $\mathcal{F} \triangleq \{\boldsymbol{\omega} : \boldsymbol{\omega} \in [-\pi, \pi]^2\}$ denote the fundamental period in the frequency domain. Now the support of $X(\boldsymbol{\omega})$ in one period can be defined as $\mathcal{X}_{\mathcal{F}} \triangleq \mathcal{X} \cap \mathcal{F}$. In addition to the common set operations such as union and intersection, we define two more operations on the point sets here, namely the shift $\mathcal{X} + \boldsymbol{c} \triangleq \{\boldsymbol{\omega} + \boldsymbol{c} : \forall \boldsymbol{\omega} \in \mathcal{X}\}$ and the linear warp $\boldsymbol{M}\mathcal{X} \triangleq \{\boldsymbol{M}\boldsymbol{\omega} : \forall \boldsymbol{\omega} \in \mathcal{X}\}$, where $\boldsymbol{c}$ is an arbitrary vector and $\boldsymbol{M}$ is a nonsingular integer matrix.

According to (1) and with the notions above, the frequency support of $Y(\boldsymbol{\omega})$ can be expressed as

$$\mathcal{Y} = \boldsymbol{M}^T \left(\bigcup_{\boldsymbol{k}\in\mathbb{N}^2} \left(\mathcal{X}_{\mathcal{F}} + 2\pi \boldsymbol{M}^{-T}\boldsymbol{k} \right) \right) \tag{2}$$

$$= \bigcup_{\boldsymbol{k}\in\mathbb{N}^2} (\boldsymbol{M}^T \mathcal{X}_{\mathcal{F}} + 2\pi\boldsymbol{k}) \tag{3}$$

In (2), we first obtain the union of all the shifted versions of $\mathcal{X}_{\mathcal{F}}$ along the grid $2\pi\boldsymbol{M}^{-T}\boldsymbol{k}$ ($\forall \boldsymbol{k} \in \mathbb{N}^2$), and then apply the linear warp $\boldsymbol{M}^T$ to get the support $\mathcal{Y}$. While in (3), $\mathcal{X}_{\mathcal{F}}$ is warped first and then shifted along the rectangular grid $2\pi\boldsymbol{k}$ ($\forall \boldsymbol{k} \in \mathbb{N}^2$). Though (2) and (3) are equivalent in describing the same decimation process, it might be more convenient to use one interpretation than the other, depending on the problem.

Definition 2.1. *We say a support $\mathcal{X}_{\mathcal{F}}$ allows aliasfree $\boldsymbol{M}$-fold decimation, if there is no overlap between all shifted versions of the support, i.e.*

$$(\mathcal{X}_{\mathcal{F}} + 2\pi\boldsymbol{M}^{-T}\boldsymbol{k}) \cap (\mathcal{X}_{\mathcal{F}} + 2\pi\boldsymbol{M}^{-T}\boldsymbol{n}) = \varnothing, \forall \boldsymbol{k} \neq \boldsymbol{n}, \tag{4}$$

or equivalently,

$$(\boldsymbol{M}^T\mathcal{X}_{\mathcal{F}} + 2\pi\boldsymbol{k}) \cap (\boldsymbol{M}^T\mathcal{X}_{\mathcal{F}} + 2\pi\boldsymbol{n}) = \varnothing, \forall \boldsymbol{k} \neq \boldsymbol{n}. \tag{5}$$

Definition 2.2. *Furthermore, we say a frequency support $\mathcal{X}_{\mathcal{F}}$ can be maximally decimated by $\boldsymbol{M}$, if aside from aliasfree decimation, the support of the decimated signal also covers the whole spectrum (i.e. no "hole" left). In this case, we need*

$$\mathbb{R}^2 = \bigcup_{\boldsymbol{k}\in\mathbb{N}^2} \left(\mathcal{X}_{\mathcal{F}} + 2\pi\boldsymbol{M}^{-T}\boldsymbol{k} \right) \tag{6}$$

$$= \bigcup_{\boldsymbol{k}\in\mathbb{N}^2} (\boldsymbol{M}^T\mathcal{X}_{\mathcal{F}} + 2\pi\boldsymbol{k}) \tag{7}$$

Starting from the definition, we can get several useful properties abut maximal decimation.

Proposition 1. *Suppose $\mathcal{X}_{\mathcal{F}}$ can be maximally decimated by $\boldsymbol{M}$. For any vector $\boldsymbol{c}$, the shifted support $\mathcal{X}_{\mathcal{F}} + \boldsymbol{c}$ can also be maximally decimated by $\boldsymbol{M}$.*

Proposition 2. *For a spectrum support $\mathcal{X}_{\mathcal{F}}$ to be maximally decimated by $\boldsymbol{M}$, a necessary condition is the area of $\mathcal{X}_{\mathcal{F}}$ must equal $\frac{4\pi^2}{|det\boldsymbol{M}|}$, which is an integer fraction of $4\pi^2$.*

Proof. Suppose $\mathcal{X}_{\mathcal{F}}$ can be maximally decimated by $\boldsymbol{M}$. According to Definition 2.2, the 2π periodically shifted versions of $\boldsymbol{M}^T\mathcal{X}_{\mathcal{F}}$ do not overlap with each other and their union completely covers the whole spectrum. This implies

$$\text{area}(\boldsymbol{M}^T\mathcal{X}_{\mathcal{F}}) = \text{area}(\mathcal{F}) \quad \Rightarrow \quad |\det(\boldsymbol{M})| \cdot \text{area}(\mathcal{X}_{\mathcal{F}}) = 4\pi^2 \tag{8}$$

$$\Rightarrow \quad \text{area}(\mathcal{X}_{\mathcal{F}}) = \frac{4\pi^2}{|\det(\boldsymbol{M})|} \tag{9}$$

Since $\boldsymbol{M}$ is an integer matrix, the area of $\mathcal{X}_{\mathcal{F}}$ must be an integer fraction of $4\pi^2$. □

As an important corollary of the above proposition, we now know it is impossible to find a critically sampled filter bank system achieving the frequency decomposition of contourlets shown in Fig. 1(b). Actually it is easy to verify that the area of any directional bandpass region in the figure is $3\pi^2/(4^m \cdot 2^n)$, where $m = 0, 1, \ldots$ corresponds to the multiresolution level, while $n = 1, 2, \ldots$ corresponds to the number of directions in that level. We can see no matter what values of m, n are we choosing, the factor 3 in the nominator can never be cancelled out and the area is not an integer fraction of $4\pi^2$. Due to Proposition 2, these shapes cannot be maximally decimated by any integer matrix.

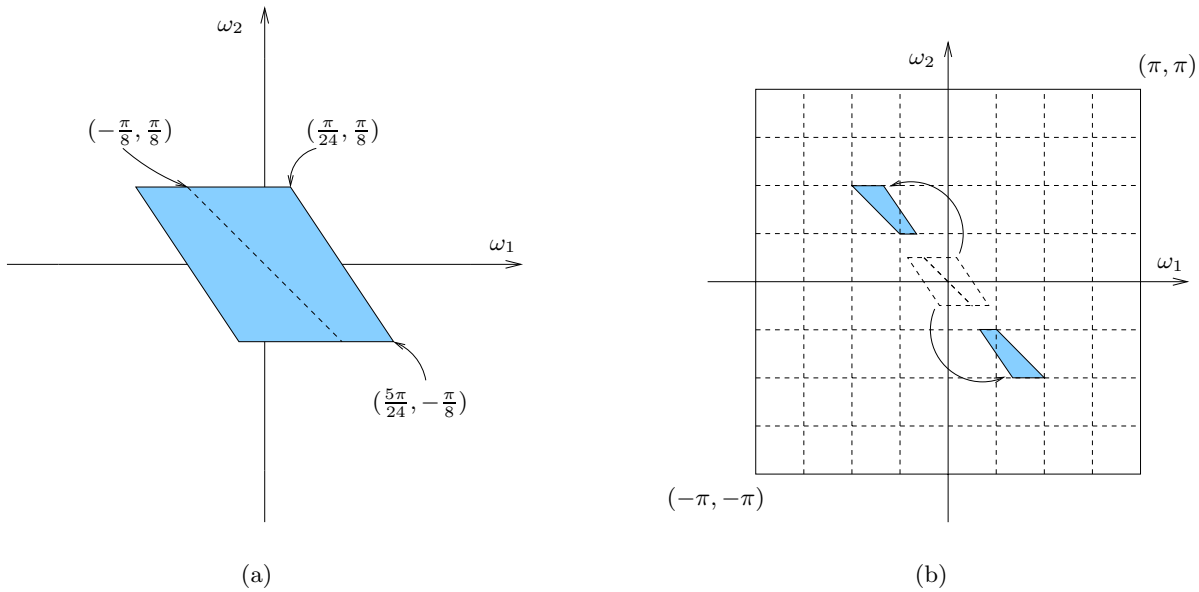

Figure 3. The pictorial explanation of Proposition 3. (a) The gray region is the original parallelogram support $\mathcal{X}_{\mathcal{F}}$, which can be maximally decimated by a matrix $\boldsymbol{M}$. (b) $\mathcal{X}_{\mathcal{F}}$ is split into two pieces. One piece is moved upwards by a shift of $(-\frac{3\pi}{8}, \frac{3\pi}{8})^T$, and the other is moved downwards by a shift of $(\frac{3\pi}{8}, -\frac{3\pi}{8})^T$. Since the shift satisfies the condition in Proposition 3, the new "split-and-shifted" support can still be maximally decimated by $\boldsymbol{M}$.

This prompts us to consider the frequency division for CRISP-contourlets as shown in Fig. 2. Here, each directional frequency region of the contourlet transform is further partitioned into 3 smaller ones, each with an area as the integer fraction of $4\pi^2$.

Since Proposition 2 is just a necessary condition, we still need to find out whether the frequency shapes in the CRISP-contourlets can really be maximally decimated. We will show this by directly finding the suitable maximal decimation matrix $\boldsymbol{M}$. The following proposition will greatly facilitate the search for $\boldsymbol{M}$.

Proposition 3. *Suppose a frequency shape $\mathcal{X}_{\mathcal{F}}$ can be maximally decimated by $\boldsymbol{M}$. If we arbitrarily divide $\mathcal{X}_{\mathcal{F}}$ into n pieces and shift each piece via a different vector $\boldsymbol{c} + 2\pi\boldsymbol{M}^{-T}\boldsymbol{k}_i$, where $\{\boldsymbol{k}_i \in \mathbb{N}^2\}_{i=1}^n$ and $\boldsymbol{c}$ is a constant vector, then the new "split and shifted" support is also maximally decimated by $\boldsymbol{M}$.*

We will explain this proposition pictorially. In Fig. 3(a), the gray support region is a parallelogram defined as

$$\mathcal{X}_{\mathcal{F}} = \left\{ \begin{pmatrix} -1/12 & 1/8 \\ 1/8 & 0 \end{pmatrix} \pi\boldsymbol{x}, \forall \boldsymbol{x} \in [-1, 1)^2 \right\}.$$

Clearly $\mathcal{X}_{\mathcal{F}}$ can be maximally decimated by a diagonal matrix $\boldsymbol{M} = \mathrm{diag}(8, 8)$. In Fig 3(b), we divide $\mathcal{X}_{\mathcal{F}}$ into two pieces and shift them along the grid $2\pi\boldsymbol{M}^{-T}\boldsymbol{k}$ (shown as dashed lines) plus a constant vector $\boldsymbol{c} = (-\pi/8, \pi/8)$. From Proposition 1, the value of $\boldsymbol{c}$ does not really matter and we can just assume $\boldsymbol{c} = \boldsymbol{0}$ for simplicity. The fact that $\mathcal{X}_{\mathcal{F}}$ can be maximally decimated by $\boldsymbol{M}$ means the shifts of $\mathcal{X}_{\mathcal{F}}$ along the grid do not overlap with each other and their union covers the whole plane. Now we just put the new "split-and-shifted" support under the same operation and clearly the shifts of it still do not overlap and their union still covers the whole plane ($\mathbb{R}^2$).

The reader might notice that the new support is actually one of the directional bandpass regions of CRISP-contourlets in Fig. 2, and now we know it can be maximally decimated by a diagonal matrix $\mathrm{diag}(8, 8)$. Similarly, we can show the following proposition.

Proposition 4. *All the directional bandpass supports in CRISP-contourlets can be maximally decimated by*

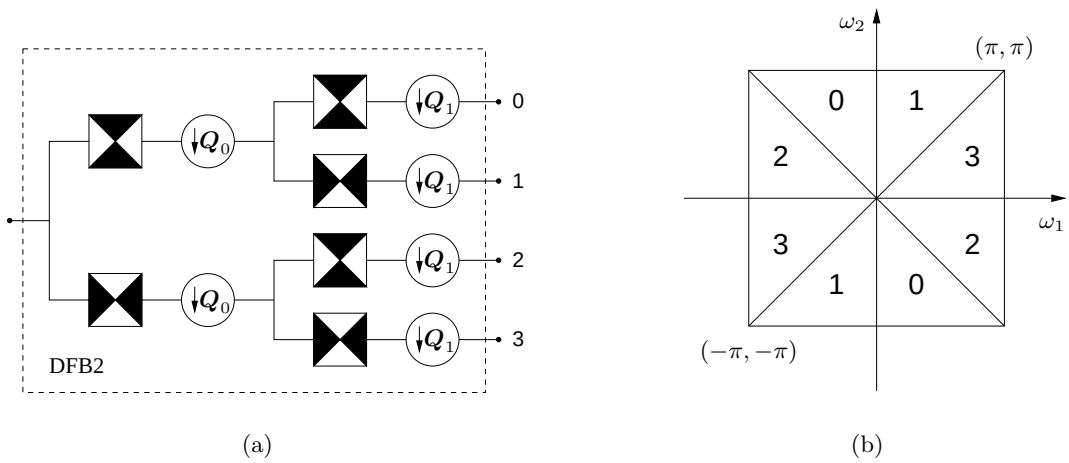

(a) (b)

Figure 4. The first two levels of CRISP-contourlets. (a) Block diagram. They are two cascaded quincunx filter banks. (b) The equivalent frequency decomposition. The whole spectrum is divided into 4 directional regions.

diagonal matrices with the following general forms.

$$\boldsymbol{M}_v^{(m,n)} = \begin{pmatrix} 2^{m+n+2} & 0 \\ 0 & 2^{m+2} \end{pmatrix} \quad \textit{and} \quad \boldsymbol{M}_h^{(m,n)} = \begin{pmatrix} 2^{m+2} & 0 \\ 0 & 2^{m+n+2} \end{pmatrix}, \tag{10}$$

where $\boldsymbol{M}_v^{(m,n)}$ *and* $\boldsymbol{M}_h^{(m,n)}$ *correspond to the principally vertical and horizontal regions respectively, while* $m = 0, 1, \ldots$ *corresponds to the multiresolution level, and* $n = 0, 1, \ldots$ *corresponds to the number of directions on that level.*

3. THE CRISP-CONTOURLETS SYSTEM

With the assurance that the frequency division of CRISP-contourlets is feasible, the next question is just how to find iterated filter banks to achieve that. In this section, we will go through the details of the system. First, the decimation matrices used in the system are as follows.

$$\boldsymbol{Q}_0 = \begin{pmatrix} 1 & -1 \\ 1 & 1 \end{pmatrix}, \quad \boldsymbol{Q}_1 = \begin{pmatrix} 1 & 1 \\ -1 & 1 \end{pmatrix}, \quad \boldsymbol{D}_0 = \begin{pmatrix} 2 & 0 \\ 0 & 1 \end{pmatrix}, \quad \boldsymbol{D}_1 = \begin{pmatrix} 1 & 0 \\ 0 & 2 \end{pmatrix}, \quad \boldsymbol{P} = \begin{pmatrix} 2 & 0 \\ 1 & 1 \end{pmatrix},$$

where $\boldsymbol{Q}_0$ and $\boldsymbol{Q}_1$ are the *quincunx* matrices, while $\boldsymbol{D}_0, \boldsymbol{D}_1$ and $\boldsymbol{P}$ are matrices with rectangular sampling lattices. In addition, we will also use the following two resampling matrices

$$\boldsymbol{R} = \begin{pmatrix} 1 & 0 \\ -1 & 1 \end{pmatrix}, \quad \text{and} \quad \boldsymbol{H} = \begin{pmatrix} -1 & 0 \\ 0 & 1 \end{pmatrix}.$$

The first two levels of CRISP-contourlets, called DFB2, are the same as those of the directional filter bank in contourlets,[1,10] using a cascading of quincunx filter banks. Fig. 4(a) shows the block diagram. In the frequency domain, each output corresponds to one of the four directional regions in Fig. 4(b). Thanks to the symmetry among the outputs, we can focus our following discussion on just one of them (band 0). The gray region in Fig. 5(a) corresponds to the directional band 0 in the support of the input signal. After going through DFB2, it is mapped to the spectrum of output 0 in the way as shown in Fig. 5(b). We can see the support is actually doubled without changing of shape, since the equivalent decimation matrix $\boldsymbol{M} = \boldsymbol{Q}_0 \cdot \boldsymbol{Q}_1 = \mathrm{diag}(2, 2)$.

On the third level, we use a new filter bank called the sheared-checkerboard (SCB) as shown in Fig. 6(a) and Fig. 6(b). We can see from Fig. 6(c) and Fig. 6(d) that the input spectrum is effectively divided into two

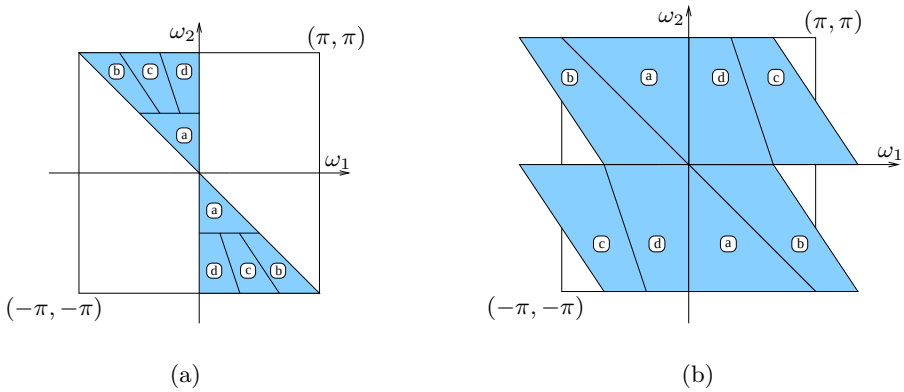

Figure 5. The frequency mapping of DFB2. (a) The gray region shows one of the directional bands in the spectrum of the input signal. (b) After DFB2, the frequency is mapped to the spectrum of output 0. The support is simply doubled without changing of shape.

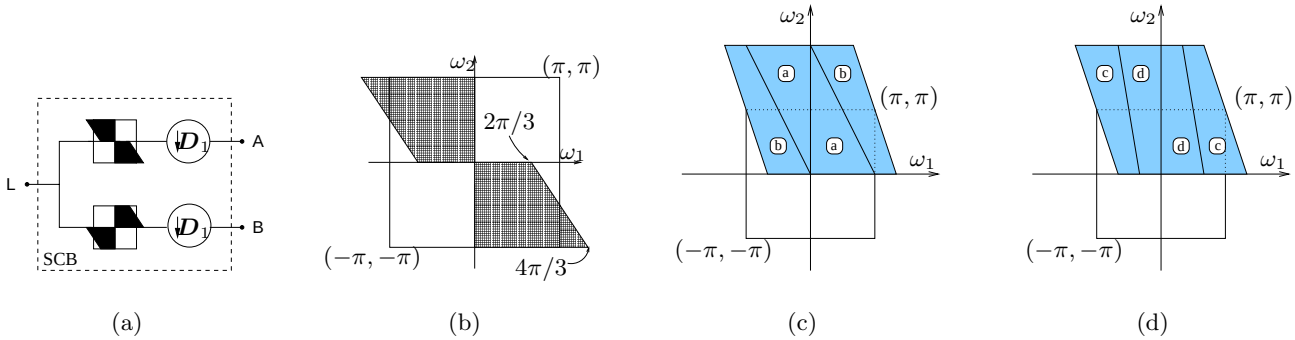

Figure 6. The sheared-checkerboard (SCB) filter bank. (a) Block diagram. (b) The spectrum support of the ideal filter. (c) The spectrum mapping at output A. (d) The spectrum mapping at output B.

groups, with the lowpass band (region (a)) and one directional highpass (region (b)) appearing at output branch A, and two other directional highpass (regions (c) and (d)) at output branch B.

Now the next step is just to further separate region (a) from (b) at branch A and separate region (c) from (d) at branch B. For the former one, it is clear that we can use the parallelogram filter bank structure as shown in Fig. 7(a) and Fig. 7(b). The two resampling matrices $\boldsymbol{R}$ and $\boldsymbol{H}$ are introduced to get the desirable frequency mapping for possible cascading. Note that they will not affect perfect reconstruction, since their effect can be cancelled out at the reconstruction filter banks by using their inverse matrices, which is also unimodular. The support region (a) comes out at the lowpass branch, while region (b) comes out at the highpass branch, with the detailed mapping shown in Fig. 7(c) and Fig. 7(d) respectively. Comparing Fig. 5(b) with Fig. 7(c), we can see that region (a) is enlarged by 2 times but still remains the original shape. Actually this is the key to multiresolution, since now we can achieve exactly the same directional frequency decomposition on the lower bands, by attaching the SCB filter bank after output L and repeating all the processes above.

To separate region (c) from (d), we can use the sheared-parallelogram (SPR) filter bank (Fig. 8(a) and Fig. 8(b)). Again, the frequency mappings in both branches are shown in Fig. 8(c) and Fig. 8(d). From the figure, we find that region (d) can be further divided (along the dashed line) by using the SPR filter bank, while region (c) can be further divided (along the dashed line) by using the PAR filter bank. Actually it can be shown via induction that arbitrary multiresolution and multidirectional (3×2^n) frequency decomposition can be achieved by an iterative cascading of the above filter banks, according to the following expansion rule:

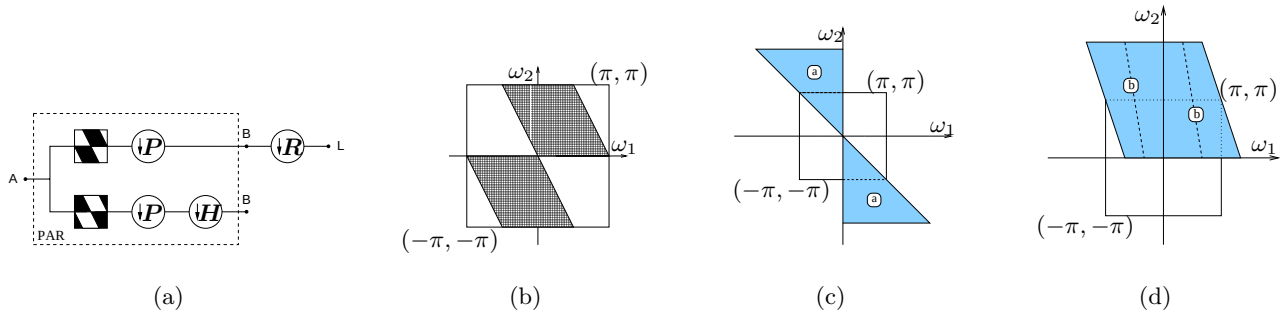

Figure 7. The parallelogram (PAR) filter bank. (a) Block diagram. (b) The spectrum support of the ideal filter. (c) The spectrum mapping at the lowpass branch. (d) The spectrum mapping at the highpass branch.

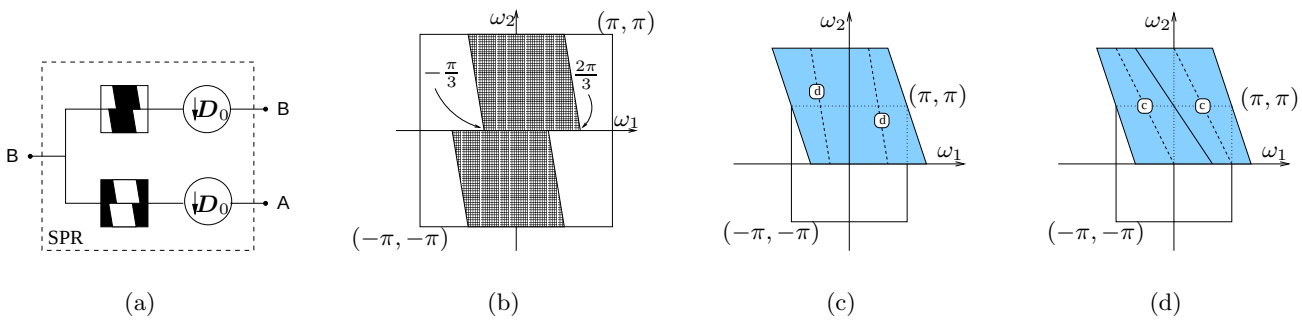

Figure 8. The sheared-parallelogram (SPR) filter bank. (a) Block diagram. (b) The spectrum support of the ideal filter. (c) The spectrum mapping at the lowpass branch. (d) The spectrum mapping at the highpass branch.

1. For multiresolution, the type "L" output is followed by the SCB filter bank, which in turn generates one type "A" and one type "B" output.
2. For multidirection, the type "A" output is followed by the PAR filter bank, which in turn generates two type "B" outputs.
3. Also for multidirection, the typed "B" output is followed by the SPR filter bank, which in turn generates one type "A" and one type "B" output.

As an example to show how these rules can be applied, we present in Fig. 9 the block diagram of the system that achieves the frequency decomposition in Fig. 2. Again, for simplicity we only give the details after one of the 4 directional branches. All other branches can be simply obtained via symmetry.

4. IMPLEMENTATION ISSUES

In this section we briefly discuss the design of the FIR filters whose spectra approximate the ideal support shapes introduced above. Totally we need to design 4 prototype filters, namely the fan, the parallelogram (PAR), the sheared-parallelogram (SPR), and the sheared-checkerboard (SCB). In practice, we will design the modulated (frequency shifted) versions of them, as shown in Fig. 10. The first two filters, i.e. fan and parallelogram, are commonly used in multidimensional systems and their design has already been studied by several authors.[11, 16, 17] Here, we will just introduce the design of the latter two filters, i.e. sheared-parallelogram and sheared-checkerboard, by using the method proposed by Tay and Kingsbury.[16] That method is based on a transformation of variable technique and can design linear phase perfect reconstruction FIR filters. The key to

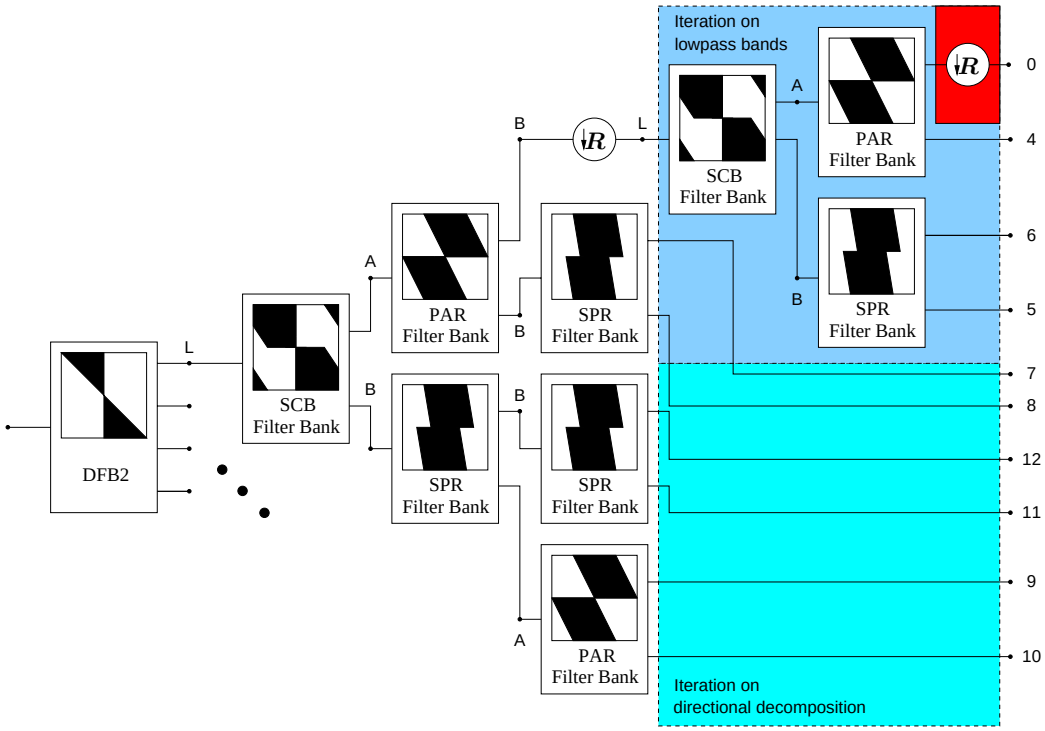

Figure 9. The block diagram of the CRISP-contourlets system achieving the frequency decomposition shown in Fig. 2.

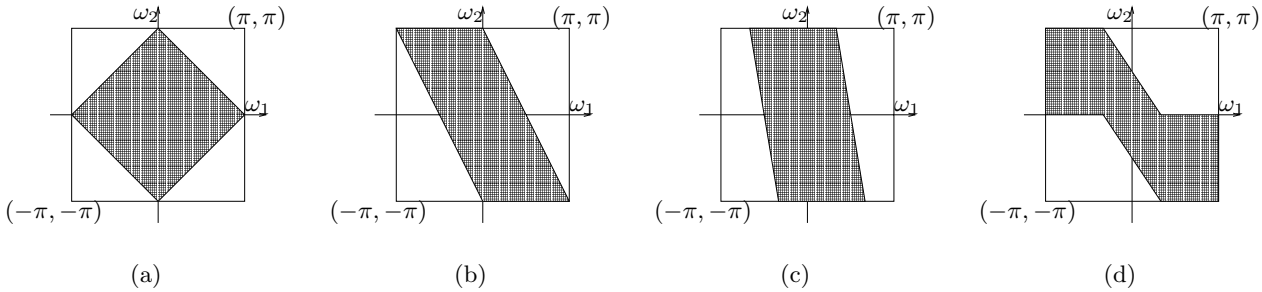

Figure 10. The modulated (frequency shifted) versions of the 4 prototype filters. (a) The fan (diamond) filter. (b) The parallelogram (PAR) filter. (c) The sheared-parallelogram (SPR) filter. (d) The sheared-checkerboard (SCB) filter.

design filters approximating the desired support shape is to get the impulse response of the ideal filter. In our case, we have

$$h_{SPR}(n_1,n_2) = sinc(\frac{n_1\pi}{2}) \cdot sinc(n_2\pi - \frac{n_1\pi}{6}), \tag{11}$$

and

$$h_{SCB}(n_1,n_2) = sinc(\frac{n_2\pi}{2}) \cdot \left(\frac{2}{3}(-1)^{n_1} \cdot sinc(\frac{n_1\pi}{3}) \cdot cos((\frac{n_1}{3}+\frac{n_2}{2})\pi) + \frac{1}{3}sinc((\frac{n_1}{3}-\frac{n_2}{2})\pi)\right), \tag{12}$$

where $h_{SPR}(n_1,n_2)$ and $h_{SCB}(n_1,n_2)$ are the impulse responses of the ideal SPR and SCB filters respectively. Finally, we show in Fig. 11 the 2-D magnitude response of the FIR filters we designed.

5. CONCLUSION

We have presented a new critically sampled directional multiresolution image representation, called CRISP-contourlets. Using an efficient iterated filter bank structure, it achieves a frequency division similar to that

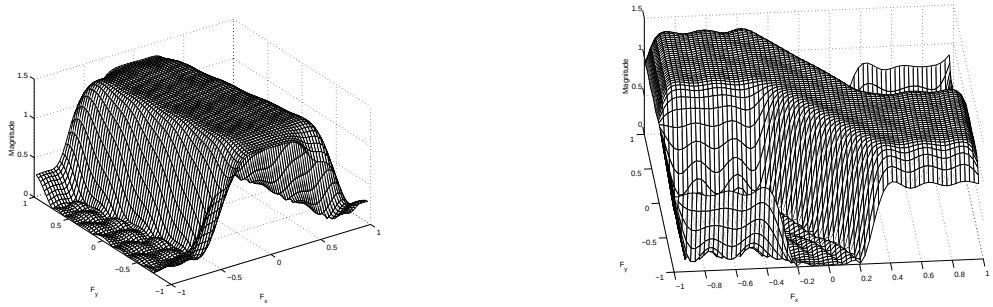

(a) (b)

Figure 11. 2-D magnitude response of the designed FIR filters. (a) The sheared-parallelogram (SPR) filter. (b) The sheared-checkerboard (SCB) filter.

of the original contourlet transform. While the added feature of nonredundant representation makes it more attractive to applications like compression. Instead of performing the multiscale and directional decomposition steps separately as is done in contourlets, the key idea here is to use a combined iterated nonseparable filter bank for both steps.

As the future research direction, we plan to investigate the regularity issue and the nonlinear approximation (NLA) behavior of the proposed system.

REFERENCES

1. M. N. Do, *Directional Multiresolution Image Representations.* PhD thesis, Swiss Federal Institute of Technology, Lausanne, Switzerland, December 2001, `http://www.ifp.uiuc.edu/~minhdo/publications/thesis.pdf`.
2. D. H. Hubel and T. N. Wiesel, "Receptive fields, binocular interaction and functional architecture in the cat's visual cortex," *Journal of Physiology* (160), pp. 106–154, 1962.
3. A. B. Watson, "The cortex transform: Rapid computation of simulated neural images," *Computer Vision, Graphics, and Image Processing* **39**(3), pp. 311–327, 1987.
4. B. A. Olshausen and D. J. Field, "Emergence of simple-cell receptive field properties by learning a sparse code for natural images," *Nature* (381), pp. 607–609, 1996.
5. E. J. Candès and D. L. Donoho, "Curvelets – a suprisingly effective nonadaptive representation for objects with edges," in *Curve and Surface Fitting*, A. Cohen, C. Rabut, and L. L. Schumaker, eds., Vanderbilt University Press, (Saint-Malo), 1999.
6. E. J. Candès and D. L. Donoho, "Curvelets, multiresolution representation, and scaling laws," in *SPIE Wavelet Applications in Signal and Image Processing VIII*, A. Aldroubi, A. F. Laine, and M. A. Unser, eds., **4119**, 2000.
7. J. P. Antoine, R. Murenzi, and P. Vandergheynst, "Directional wavelets revisited: Cauchy wavelets and symmetry detection in patterns," *Applied and Computational Harmonic Analysis* **6**, pp. 314–345, 1999.
8. F. C. A. Fernandes, R. L. van Spaendonck, and C. S. Burrus, "A directional, shift-insensitive, low-redundancy, wavelet transform," in *Proc. IEEE Int. Conf. on Image Proc.*, (Thessaloniki, Greece), Oct 2001.
9. N. Kingsbury, "Complex wavelets for shift invariant analysis and filtering of signals," *Journal of Appl. and Comput. Harmonic Analysis* **10**, pp. 234–253, 2001.
10. M. N. Do and M. Vetterli, "Contourlets: a computational framework for directional multiresolution image representation," *IEEE Trans. Image Proc.* , 2003. submitted, `http://www.ifp.uiuc.edu/~minhdo/publications`.

11. R. H. Bamberger and M. J. T. Smith, "A filter bank for the directional decomposition of images: theory and design," *IEEE Trans. Signal Proc.* **40**, pp. 882–893, April 1992.
12. P. S. Hong and M. J. T. Smith, "An octave-band family of non-redundant directional filter banks," in *Proc. IEEE Int. Conf. Acoust., Speech, and Signal Proc.*, pp. 1165–1168, (Orlando, USA), 2002.
13. E. Viscito and J. P. Allebach, "The analysis and design of multidimensional FIR perfect reconstruction filter banks for arbitrary sampling lattices," *IEEE Trans. Circ. and Syst.* **38**, pp. 29–41, Jan 1991.
14. P. P. Vaidyanathan, *Multirate Systems and Filter Banks*, Prentice Hall, 1993.
15. M. Vetterli and J. Kovačević, *Wavelets and Subband Coding*, Prentice-Hall, 1995.
16. D. B. H. Tay and N. Kingsbury, "Flexible design of multidimensional perfect reconstruction FIR 2-band filters using transformations of variables," *IEEE Trans. Image Proc.* **2**, pp. 466–480, 1993.
17. S.-M. Phoong, C. W. Kim, P. P. Vaidyanathan, and R. Ansari, "A new class of two-channel biorthogonal filter banks and wavelet bases," *IEEE Trans. Signal Proc.* **43**, pp. 649–665, Mar. 1995.